A method to detect layover and shadow based on distributed spaceborne single-baseline InSAR

REN Yun, ZOU Huanxin, ZHOU Shilin, SUN Hao and JI Kefeng
Collegeof Electronic Science and Engineering, National University of Defense Technology, Changsha, China.

E-mail: 156333408@qq.com

Abstract: Layover and Shadow are inevitable phenomenena in InSAR, which seriously destroy the continuity of interferometric phase images and present difficulties in the follow-up phase unwrapping. Thus, it's significant to detect layover and shadow. This paper presents an approach to detect layover and shadow using the auto-correlation matrix and amplitude of the two images. The method can make full use of the spatial information of neighboring pixels and effectively detect layover and shadow regions in the case of low registration accuracy. Experiment result on the simulated data verifies effectiveness of the algorithm.

1. Introduction

InSAR is an important remote sensing technique to achieve Digital Elevation Model (DEM). It has the characteristic of all-weather, all-time, long-range and high-resolution[1]. InSAR has attracted much attention all over the world since it was firstly brought forward inthe mid-17th century[2] [3].

In the past two decades, some research has been presented in the literatures about layover and/or shadow detection, phase unwrapping, DEM inversion and so on. However, they did not make full use of the information of the interferometric signal. For example, Andrew J. Wilkinson has deep research on the statistical analysis and modeling in layover and shadow regions[4]; and Liu Xiang-le has proposed resolving the layover problem using the unitary ESPIRT algorithm on the frame of multi-baseline InSAR[5]. But the data of multi-baseline InSAR is difficult to obtain.

In this paper, a method is presented to detect layover and shadow using the amplitude and auto-correlation matrix of the two images. It can make full use of the spatial information of neighboring pixels and effectively detect layover and shadow regions in the case of low registration accuracy. Experiment results on the simulated data verifyeffectiveness of the algorithm.

2. The Geometry Model and Statistical Model in Layover and shadow regions

2.1. The Geometry Model in Layover and shadow regions

Layover and shadow are ubiquitousphenomenain SAR images which are caused by the radar imaging geometrical relationship, especially in steep hills.

Layover is formed due tothe fore-slope angle θgreater than the SAR side-looking angle β, causing that the echo signal of slope top arrives SAR receiver ahead of that of slope bottom. Because there is the same distance between sensor and these regions including L_1、L_2、L_3, the back-scattered energy from these regions will overlay in the same pixel of SAR image, as depicted in figure 1.Consequently, layover manifests as bright regions in SAR images.

However, when the back-slope angle α is greater than the SAR side-looking angle β, no useful echo wave can be received by SAR receiver because the higher object will block the back-slope areas. Thus, shadow is formed by thermal noise or speckle noise. As shown in figure 1, the back-slope areas such as S, cannot return a signal message and manifests as black regions in SAR images.

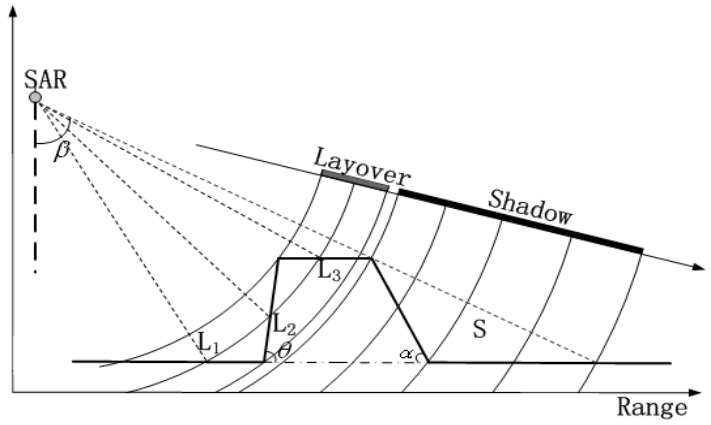

Figure 1. Sketch of layover and shadow

Through the above analysis, the echo intensity in layover is far too high relative to other homogeneous regions (usually 3 times stronger[6]) while the echo intensity in shadow is far too low relative to other homogeneous regions (usually 10^2 times weaker[6]). The SAR amplitude of layover is much higher than other regions while that of shadow is rather lower than other regions reflected in amplitude map.

2.2. The Statistical Model in Layover and shadow regions

Assuming that the SAR images are accurately coregistered and the interferometric phases are flattened. And the complex data vector, denoted as $\mathbf{S}(i)$, of a pixel pair (corresponding to the same ground area) of the coregistered SAR images can be formulated as follows:

$$\mathbf{S}(i)=\begin{bmatrix} s_1(i) \\ s_2(i) \end{bmatrix}=\begin{bmatrix} 1 \\ e^{j\varphi_i} \end{bmatrix} \odot \begin{bmatrix} x_1(i) \\ x_2(i) \end{bmatrix}+\begin{bmatrix} n_1(i) \\ n_2(i) \end{bmatrix}=\mathbf{a}(\varphi_i) \odot \mathbf{x}(i)+\mathbf{n}(i) \tag{1}$$

where $\mathbf{a}(\varphi_i)=\begin{bmatrix} 1 & e^{j\varphi_i} \end{bmatrix}^{\mathrm{T}}$ is called the spatial steering vector of the pixel pair i, $\mathbf{x}(i)$ is the complex magnitude vector (i.e., the complex reflectivity vector received by the array) of the pixel pair i, $\mathbf{n}(i)$ is the additive noise term, superscript T denotes matrix transpose, φ_i denotes the true terrain interferometric phase to be estimated, and $\odot$ denotes the Hadmard product. In(1), $\mathbf{S}(i)$ is called the spatial data vector and can be modeled as a joint zero-mean complex circular Gaussian random vector. The corresponding auto-correlation matrix, denoted as $\mathbf{R}(i)$, of $\mathbf{S}(i)$ is given by

$$\begin{aligned} \mathbf{R}(i) &= E\{\mathbf{S}(i)\mathbf{S}^H(i)\}=\mathbf{a}(\varphi_i)\mathbf{a}^H(\varphi_i) \odot E\{\mathbf{x}(i)\mathbf{x}^H(i)\}+\delta_n^2\mathbf{I} \\ &= \delta_s^2(i)\mathbf{a}(\varphi_i)\mathbf{a}^H(\varphi_i) \odot \mathbf{R}_{\mathbf{x}}(i)+\delta_n^2\mathbf{I} \end{aligned} \tag{2}$$

$$\mathbf{R}_{\mathbf{x}}(i)=\begin{bmatrix} r_{11}(i) & r_{12}(i) \\ r_{21}(i) & r_{22}(i) \end{bmatrix} \tag{3}$$

where $\mathbf{R}_{\mathbf{x}}(i)$ is called the correlation coefficient matrix of the pixel pair i, $\mathbf{I}$ is a 2×2 identity matrix, $r_{mn}(i)$ ($0 \leqslant r_{mn}(i) \leqslant 1$, m=1,2 and n=1,2) are the correlation coefficients of the pixel pair i between the satellites m and n, $E\{\}$ denotes the statistical expectation, superscript H denotes vector conjugate-transpose, δ_s^2 is the echo power of the pixel pair i and δ_n^2 is the noise power.

In practice, the statistical auto-correlation matrix given by(2) can be estimated by the corresponding sample auto-correlation matrix of independent and identically distributedsamples[7]. The independent and identically distributed samples can be obtained under the assumptions that the neighboring pixels have an identical spatial steering vector (i.e., an identical terrain height) and the complex reflectivity is independent from pixel to pixel.

3. Layover and Shadow detection based on the auto-correlation matrix

3.1. The estimation of auto-correlation matrix

In practice, the desired pixel pair and its neighboring pixel pairs are used to jointly perform the auto-correlation matrix estimation. An example to formulate the joint data vector, denoted by $\mathbf{Si}(i)$, is shown in figure 2, where circles represent SAR image pixels and *i* denotes the centric pixel pair[7].

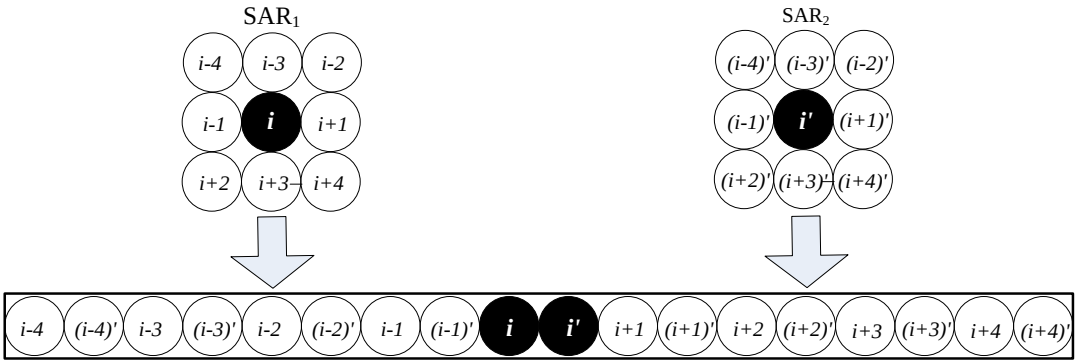

Figure 2. Formulation of joint data vector using a 3×3 pixel pair window

The joint data vector $\mathbf{Si}(i)$, shown in figure 2, can be formulated as

$$\mathbf{Si}(i)=[\mathbf{s}(i-4)^{\mathrm{T}},\ \mathbf{s}(i-3)^{\mathrm{T}},\ \ldots,\ \mathbf{s}(i)^{\mathrm{T}},\ \ldots,\ \mathbf{s}(i+3)^{\mathrm{T}},\ \mathbf{s}(i+4)^{\mathrm{T}}]^{\mathrm{T}} \tag{4}$$

which implies that the number of the neighboring pixel pairs is 8, and $\mathbf{Si}(i)$ is a 18×1 vector. The corresponding joint auto-correlation matrix is given by

$$\mathbf{R}(i)=E\{\mathbf{Si}(i)\cdot\mathbf{Si}^{H}(i)\}=\mathbf{a}(\boldsymbol{\varphi})\mathbf{a}^{H}(\boldsymbol{\varphi})\otimes\mathbf{R}_{\mathbf{xi}}(i)+\delta_n^2\mathbf{I} \tag{5}$$

where $\mathbf{a}(\boldsymbol{\varphi})=[\mathbf{a}^{\mathrm{T}}(\varphi_{i-4}),\ \mathbf{a}^{\mathrm{T}}(\varphi_{i-3}),\ \ldots,\ \mathbf{a}^{\mathrm{T}}(\varphi_{i+4})]^{\mathrm{T}}$ and $\mathbf{R}_{\mathbf{xi}}(i)$ are referred to as the joint array steering vector and the joint correlation function matrix of the pixel pair *i* respectively.

Under these assumptions that the neighboring pixels have an identical terrain height., the array steering vectors of the pixel pairs in $\mathbf{Si}(i)$ become identical, i.e.,

$$\mathbf{a}(\varphi_{i-4})=\mathbf{a}(\varphi_{i-3})=\ldots=\mathbf{a}(\varphi_{i+4})=\begin{bmatrix}1 & \mathrm{e}^{j\varphi_i}\end{bmatrix}^{\mathrm{T}} \tag{6}$$

In the sense of statistical expectation, $\mathbf{R}_{\mathbf{xi}}(i)$ only have signal components, which can be eigen-decomposed into

$$\mathbf{R}_{\mathbf{xi}}(i)\overset{\mathrm{EVD}}{=}\sum_{k=1}^{\mathrm{K}}\lambda_r^{(k)}\cdot\boldsymbol{\beta}_r^{(k)}\cdot\boldsymbol{\beta}_r^{(k)H} \tag{7}$$

where K is the number of the principal eigenvalues $\lambda_r^{(k)}$ (k = 1,2,…,K)of $\mathbf{R}_{\mathbf{xi}}(i)$, and $\boldsymbol{\beta}_r^{(k)}$ are the corresponding eigenvectors. If we substitute(7) into(5), then(5) becomes

$$\begin{aligned}\mathbf{R}(i)&=\mathbf{a}(\boldsymbol{\varphi})\mathbf{a}^{H}(\boldsymbol{\varphi})\otimes\sum_{k=1}^{\mathrm{K}}\lambda_r^{(k)}\cdot\boldsymbol{\beta}_r^{(k)}\cdot\boldsymbol{\beta}_r^{(k)H}+\delta_n^2\mathbf{I}\\&=\sum_{k=1}^{\mathrm{K}}\lambda_r^{(k)}\cdot(\mathbf{a}(\boldsymbol{\varphi})\otimes\boldsymbol{\beta}_r^{(k)})\cdot(\mathbf{a}(\boldsymbol{\varphi})\otimes\boldsymbol{\beta}_r^{(k)})^{H}+\delta_n^2\mathbf{I}\end{aligned} \tag{8}$$

It is evident that $\mathbf{a}(\varphi)\otimes\boldsymbol{\beta}_r^{(k)}$ are orthogonal to each other under the definition of $\mathbf{a}(\varphi)$, which implies that the joint signal subspace can be spanned by $\mathbf{a}(\varphi)\otimes\boldsymbol{\beta}_r^{(k)}$. $\mathbf{R}(i)$ of(8) can be eigen-decomposed into

$$\begin{aligned}\mathbf{R}(i) &= \sum_{k=1}^{\mathrm{K}} \lambda_r^{(k)} \cdot (\mathbf{a}(\varphi)\otimes\boldsymbol{\beta}_r^{(k)}) \cdot (\mathbf{a}(\varphi)\otimes\boldsymbol{\beta}_r^{(k)})^H + \delta_n^2\mathbf{I} \\ &= \sum_{k=1}^{\mathrm{K}} (\lambda_r^{(k)} + \delta_n^2) \cdot \boldsymbol{\beta}_{rx}^{(k)} \cdot \boldsymbol{\beta}_{rx}^{(k)\,H} + \sum_{l=1}^{18-\mathrm{K}} \delta_n^2 \cdot \boldsymbol{\beta}_n^{(l)} \cdot \boldsymbol{\beta}_n^{(l)H}\end{aligned} \tag{9}$$

where $\boldsymbol{\beta}_{rx}^{(k)}$ are the principal eigenvectors of $\mathbf{R}(i)$ that span the same joint signal subspace as spanned by $\mathbf{a}(\varphi)\otimes\boldsymbol{\beta}_r^{(k)}$, and $\boldsymbol{\beta}_n^{(l)}$ (l = 1,2,…,18-K) are the corresponding noise eigenvectors of $\mathbf{R}(i)$ that span the joint noise subspace.

As we know, the correlation coefficient from different regions is different including layover and shadow regions[8][9]. Because the signal from shadow is approximated at Gaussian noise, the correlation coefficient reaches zero. Meanwhile the correlation coefficient of a layover can be expressed the weight sum of the correlation coefficient of each overlap area. There is a close relationship between the correlation coefficient and the eigenvalue clustering of joint auto-correlation matrix, which can be used to detect layover and shadow. The number of the large eigenvalues of joint auto-correlation matrix is same as the number of the overlap signal of the pixel *i*. In ideal circumstances, all the eigenvalues of joint auto-correlation matrix are noise eigenvalues in shadow.

3.2. Layover and Shadow detection based on the eigenvalues clustering of auto-correlation matrix

In practice, the ideal eigenvalue clustering of joint auto-correlation matrix is hard to achieve because of the coregistration error, additive noise or multiplicative noise. A common solution is to use the estimation of the signal number based on information theory. Some conventional criterions include Akaike Information Criterion (AIC), Minimum Description Length (MDL) criterion and Efficient Detection Criterion (EDC)[10].

This paper chooses the AIC, given by

$$\mathrm{AIC}(n_s) = 2\cdot \mathrm{P}\cdot(\mathrm{M}-n_s+1)\cdot \ln\Delta(n_s) + 2\cdot(n_s-1)\cdot(2\mathrm{M}-n_s+1) \tag{10}$$

where P is the multilook number and $\Delta(\bullet)$ is a likelihood function defined as

$$\Delta(n_s) = \frac{\dfrac{1}{\mathrm{M}-n_s+1}\cdot\sum_{i=n_s}^{\mathrm{M}}\lambda_i}{\left(\prod_{i=n_s}^{\mathrm{M}}\lambda_i\right)^{\frac{1}{\mathrm{M}-n_s+1}}} \tag{11}$$

where M is the number of all eigenvalues of joint auto-correlation matrix $\mathbf{R}(i)$ and λ_i is one of the eigenvalues. n_s is the number of the eigenvalue to be estimated.

Then

$$\dim(\mathrm{R}) = \min_{n_s=1,\ldots,\mathrm{M}} \mathrm{AIC}(n_s) \tag{12}$$

which represents the dimension of the signal subspace (i.e., the signal number).

This paper estimates the joint auto-correlation matrix pixel by pixel and then uses the above-mentioned AIC to detect layover and shadow. The results have showed that we can define a threshold (such as two) forthe signal number. If the signal number is greater than two, the pixel *i* is discriminated the pixel from layover region.If the signal number is less than two, the pixel *i* is discriminated the pixel from shadow region. And in other cases, the pixel *i* is discriminated the pixel from normal region.

3.3. Experiment Procedures

The algorithm flow chart is shown in figure 3 through above theoretical analysis.

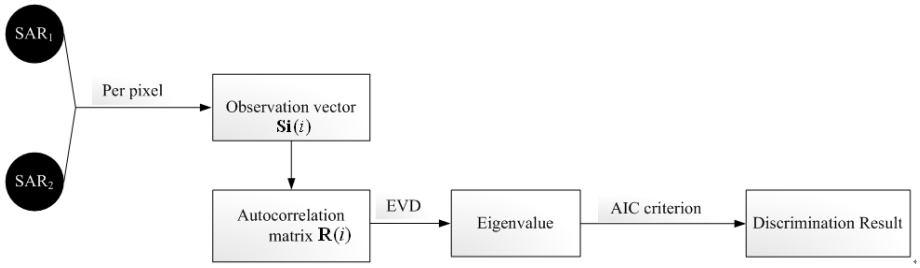

Figure 3. The algorithm flow chart

4. Simulation Experiment

Due to the difficulty of obtaining the real InSAR data, this paper performs an experiment with the crater data simulated by Space-Borne Radar Advanced System. The image size is 1085×850 pixels.

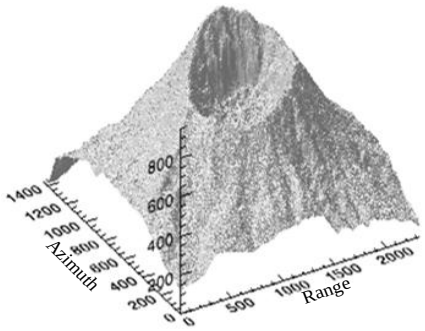

Figure 4.DEM of the crater

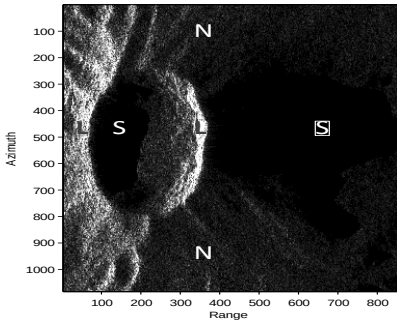

Figure 5. Amplitude of the crater

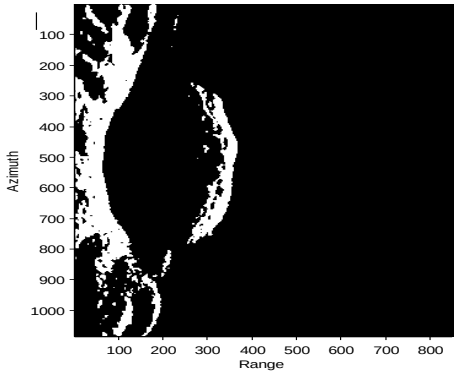

Figure 6. Detection result of Layover

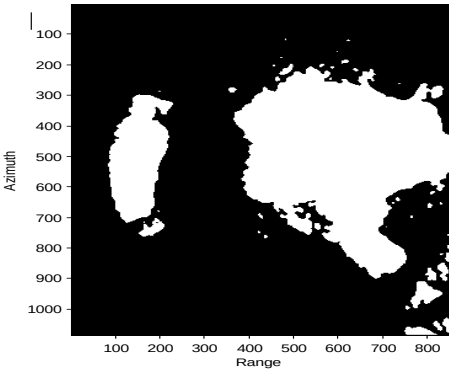

Figure 7. Detection result of Shadow

The simulated crater,whose altitude is less than 951 meters,originates SRTM measured data and its DEM is shown in figure 4. The interferometry amplitude of the crater is shown in figure 5 in which layover and shadow regions have been marked with the word L or S respectively.

Table1. The comparison of false ratesin layover and shadow

method	Layover	Shadow
reference [3]	81.7%	79.6%
reference [5]	82.3%	89.5%
this paper	90.4%	93.1.7%

The detection results of layover and shadow are shown in figure 6 and figure 7 respectively where the white areas are the pixels belonging to layover or shadow. The results imply that layover and shadow can be detected effectively by the proposed method in this paper, which is also verified compared with other methods shown in table.1.

5. Conclusions

This paper analyzes the feasibility of experiment in theory in the first place. Then the effectiveness of experiment is validated by simulation. The experiment result implies that layover and shadow can be detected effectively by the method above, which has provided the reliable basis for the following InSAR processing. The next step is going to apply the method in the realmeasurement data to enhance the engineering practicality.

6. References

[1] Rosen P A, Hensley S. Synthetic aperture radar interferometry. 2000*Proc.IEEE*.**88**333-382.
[2] Wang Chao,Zhang Hong, Liu Zhi, 2002 *Space-Borne Synthetic Aperture Radar Interferometry*. (Beijing: Science Press)
[3] Wang Jian, Xiang MaoSheng, Li Shao'en. A Method for Extracting the SAR Shadow from InSAR Coherence. 2005*Geomatics and Information Science of Wuhan University*.**30**12.
[4] A J Wilkinson. Synthetic aperture radar interferometry: a model for the joint statistics in Layover areas. 1998*IEEE Proceedings of the 1998 South African Symposium on Communications and Signal Processing*. **98**333-338.
[5] Liu Xiangle, Song Yuepeng, Yang Ruliang. Layover Solution Based On Unitary ESPRIT Algorithm in Multi-baseline InSAR. 2008*Journal of Electronics andInformation Technology*.**30**7.
[6] Sun Zaoyu. Study on Signal Simulating and Processing of Distributed Spaceborne Interferometric SAR System.*A dissertation for the degree of Doctor of NUDT*, Changsha, China, 2007
[7] Li Zhen Fang, Bao Zhen, Li H. Image auto-coregistration and InSAR interferogram estimation using joint subspace projection. 2006*IEEE Trans on GRS*.**44**251-260
[8] Liu Zilong. Study on Signal processing Technique of Spaceborne InSAR.*A thesis for the degree of Master of NUDT*, Changsha, China, 2009
[9] Cai Bin. Research on Signal Processing of Distributed Spaceborne InSAR and SAR-GMTI. *A dissertation for the degree of Doctor of NUDT*, Changsha, China, 2009
[10] F Gatelli, A Monti Guarnieri. The wavenumber shift in SAR interferometry. 1994*Transactions on Geoscience and Remote Sensing*.**32**855-865.